the mandibles on the basis of tooth structure. They show that the skull was flat-snouted, as in panderichthyids and early tetrapods; unlike the skull of *Panderichthys* (my unpublished observation), they carry a tetrapod-like ornament of radially arranged, irregular pits and ridges.

The Scat Craig tibia represents the earliest known tetrapod-type hindlimb, the jaws belong to an animal apparently more closely related to tetrapods than *Panderichthys* or any other known fish, and the humerus possesses a suite of tetrapod characters. It is tempting to assume that they are parts of the same organism; their sizes are compatible, and the number of jaw fragments is large enough to suggest that the apparent absence of more than one tetrapod-like form is not due to sampling error. But although the tibia clearly belongs to a leg, the humerus differs enough from the early tetrapod pattern to make it uncertain whether the appendage carried digits or a fin. At first sight the combination of two such extremities in one animal seems highly unlikely on functional grounds. If, however, tetrapod limbs evolved for aquatic rather than terrestrial locomotion, as recently suggested[35,36], such a morphology might be perfectly workable. Note that the forelimb of *Acanthostega*[16] is more fish-like than the hindlimb and could probably not be brought into a weight-bearing position. Regrettably, the fragmentary nature of the Scat Craig material makes it impossible to determine whether the tibia and humerus really belong together, or with the jaws; it does show, however, that tetrapods or very tetrapod-like animals had appeared before the end of the Frasnian. □

Received 26 July; accepted 14 October 1991.

1. Säve-Söderbergh, G. *Meddr. Grønland* **94,** 1–107 (1932).
2. Jarvik, E. *Basic Structure and Evolution of Vertebrates* vol. 1 (Academic, London, 1980).
3. Lebedev, O. A. *Dokl. Akad. Nauk SSSR* **278,** 1407–1473 (1984).
4. Campbell, K. S. W. & Bell, M. W. *Alcheringa* **1,** 369–381 (1977).
5. Warren, J. W. & Wakefield, N. A. *Nature* **238,** 469–470 (1972).
6. Warren, A., Jupp, R. & Bolton, B. *Alcheringa* **10,** 183–186 (1986).
7. Vorobyeva, E. I. *Trudy paleont. Inst.* **163,** 1–239 (1977).
8. Schultze, H.-P. & Arsenault, M. *Palaeontology* **28,** 293–309 (1985).
9. Schultze, H.-P. *J. Morph.* (suppl. 1) 39–74 (1987).
10. Ahlberg, P. E. *Zool. J. Linn. Soc.* (in the press).
11. Vorobyeva, E. I. *Neues Jb. Geol. Paläont. Mh.* **1975,** 315–320 (1975).
12. Tarlo, L. B. *Q. Jl geol. Soc. Lond.* **117,** 193–213 (1961).
13. Miles, R. S. *Palaeontogr. Soc. (Monogr.)* **552,** 1–130 (1968).
14. House, M. R. *et al. Spec. Rep. Geol. Soc. Lond.* **8,** 1–110 (1977).
15. Harland, W. B. *et al. A Geologic Time Scale* (Cambridge University Press, 1982).
16. Coates, M. I. & Clack, J. A. *Nature* **347,** 66–69 (1990).
17. Gaffney, E. S. *Bull. Carnegie Mus. nat. Hist.* **13,** 92–105 (1979).
18. Panchen, A. L. & Smithson, T. R. *Biol. Rev.* **62,** 341–438 (1987).
19. Godfrey, S. J. *Phil. Trans. R. Soc.* B**323,** 75–133 (1989).
20. Holmes, R. *Phil. Trans. R. Soc.* B**306,** 431–527 (1984).
21. Panchen, A. L. *Phil. Trans. R. Soc.* B**309,** 505–568 (1985).
22. Smithson, T. R. *Zool. J. Linn. Soc.* **85,** 317–410 (1985).
23. Andrews, S. M. & Westoll, T. S. *Trans. R. Soc. Edinb.* **68,** 207–329 (1970).
24. Rackoff, J. S. in *The Terrestrial Environment and the Origin of Land Vertebrates* (ed. Panchen, A. L.) 255–292 (Academic, London, 1980).
25. Long, J. A. *Palaeontology* **30,** 839–852 (1987).
26. Andrews, S. M. & Westoll, T. S. *Trans. R. Soc. Edinb.* **68,** 391–489 (1970).
27. Ahlberg, P. E. *Zool. J. Linn. Soc.* **96,** 119–166 (1989).
28. Schultze, H.-P. *Palaeontogr. Ital.* **65,** 59–137 (1969).
29. Jessen, H. *Ark. Zool.* **18**(2), 305–389 (1966).
30. Gross, W. *Abh. preuss. Akad. Wiss. Math.-naturw. Kl.* **1941,** 1–51 (1941).
31. Smithson, T. R. *Palaeontology* **23,** 915–923 (1980).
32. Smithson, T. R. *Zool. J. Linn. Soc.* **76,** 29–90 (1982).
33. Godfrey, S. J. & Holmes, R. B. *Can. J. Earth. Sci.* **26,** 1036–1040 (1989).
34. Vorobyeva, E. I. *Trudy. Paleont. Inst.* **104,** 1–108 (1962).
35. Edwards, J. L. *Am. Zool.* **29,** 235–254 (1989).
36. Coates, M. I. & Clack, J. A. *Nature* **352,** 234–235 (1991).

ACKNOWLEDGEMENTS. I thank P. L. Forey, S. M. Andrews and H. C. Ivimey-Cook for lending me Scat Craig specimens in their care, O. A. Lebedev for helpful comments on the material and access to the *Obruchevichthys* specimens in the Palaeontological Institute, Moscow, K. S. W. Campbell for allowing me to examine the only known specimen of *Metaxygnathus* and J. A. Clack and M. I. Coates for access to the *Acanthostega* material, and for criticizing a previous version of this paper.

Primary structure and functional expression of a developmentally regulated skeletal muscle chloride channel

Klaus Steinmeyer, Christoph Ortland & Thomas J. Jentsch*

Centre for Molecular Neurobiology (ZMNH), Hamburg University, Martinistrasse 52, D-2000 Hamburg 20, Germany

SKELETAL muscle is unusual in that 70–85% of resting membrane conductance is carried by chloride ions[1]. This conductance is essential for membrane-potential stability, as its block by 9-anthracene-carboxylic acid and other drugs causes myotonia[2,3]. Fish electric organs are developmentally derived from skeletal muscle, suggesting that mammalian muscle may express a homologue of the *Torpedo mamorata* electroplax chloride channel[4,5]. We have now cloned the complementary DNA encoding a rat skeletal muscle chloride channel by homology screening to the Cl^- channel from *Torpedo*[4] (Fig. 1*a*). It encodes a 994-amino-acid protein which is about 54% identical to the *Torpedo* channel and is predominantly expressed in skeletal muscle. Messenger RNA amounts in that tissue increase steeply in the first 3–4 weeks after birth, in parallel with the increase in muscle Cl^- conductance[6]. Expression from cRNA in *Xenopus* oocytes leads to 9-anthracene-carboxylic acid-sensitive currents with time and voltage dependence typical for macroscopic muscle Cl^- conductance. This and the functional destruction of this channel in mouse myotonia[7] suggests that we have cloned the major skeletal muscle chloride channel.

We have called the cloned channel ClC−1 to distinguish it from the *Torpedo* channel (ClC-0)[4] and a recently cloned different mammalian Cl^- channel, ClC-2 (A. Thiemann, S. Gründer, M. Pusch and T.J.J., manuscript in preparation). The predicted protein (994 amino acids, relative molecular mass 110,000 (M_r, 110K)) is larger than the *Torpedo* Cl^- channel (~89K)[4]. This is due to amino- and carboxy-terminal extensions and to an insertion between domains D12 and D13. Hydropathy analysis[8] (Fig. 1*b*) suggests a topology similar to the *Torpedo* Cl^- channel. The greatest homology with the *Torpedo* protein is in putative membrane spans and adjacent regions. There is also considerable conservation of D13, which, by hydropathy, is a poor candidate for a transmembrane segment. This suggests that D13 is functionally important. Indeed, truncating the *Torpedo* channel between D12 and D13 renders it nonfunctional in the oocyte (K.S., C. Schmekal and T.J.J., unpublished observation).

The tissue distribution of ClC-1 was examined by northern analysis (Fig. 2*a*). A prominent band of about 4.5 kilobases (kb) was present in skeletal muscle. Faint bands of identical size were detected in kidney, liver, heart and in the smooth muscle cell line A10 (ref. 9). Thus, ClC-1 is predominantly, but probably not exclusively, expressed in skeletal muscle.

In rats, muscle Cl^- conductance increases steeply during the first few weeks after birth[6]. ClC-1 mRNA amounts in muscle increase rapidly between days 1 and 30 after birth (Fig. 2*b*), suggesting a rise in channel density as the primary mechanism of postnatal conductance increase. Developmental changes in expression are also known for other muscle channels[10–15], possibly suggesting similar mechanisms of regulation.

Injection of ClC-1 cRNA into oocytes leads to functional expression of Cl^- channels open under resting conditions, thereby clamping the oocyte membrane to the chloride equilibrium potential (−20 to −30 mV). Conductance is nearly linear between −80 and −20 mV, but decreases at more positive values (Fig. 3). At voltages more negative than about −80 mV, currents become progessively time-dependent. Hyperpolarizing voltage

* To whom correspondence should be addressed.

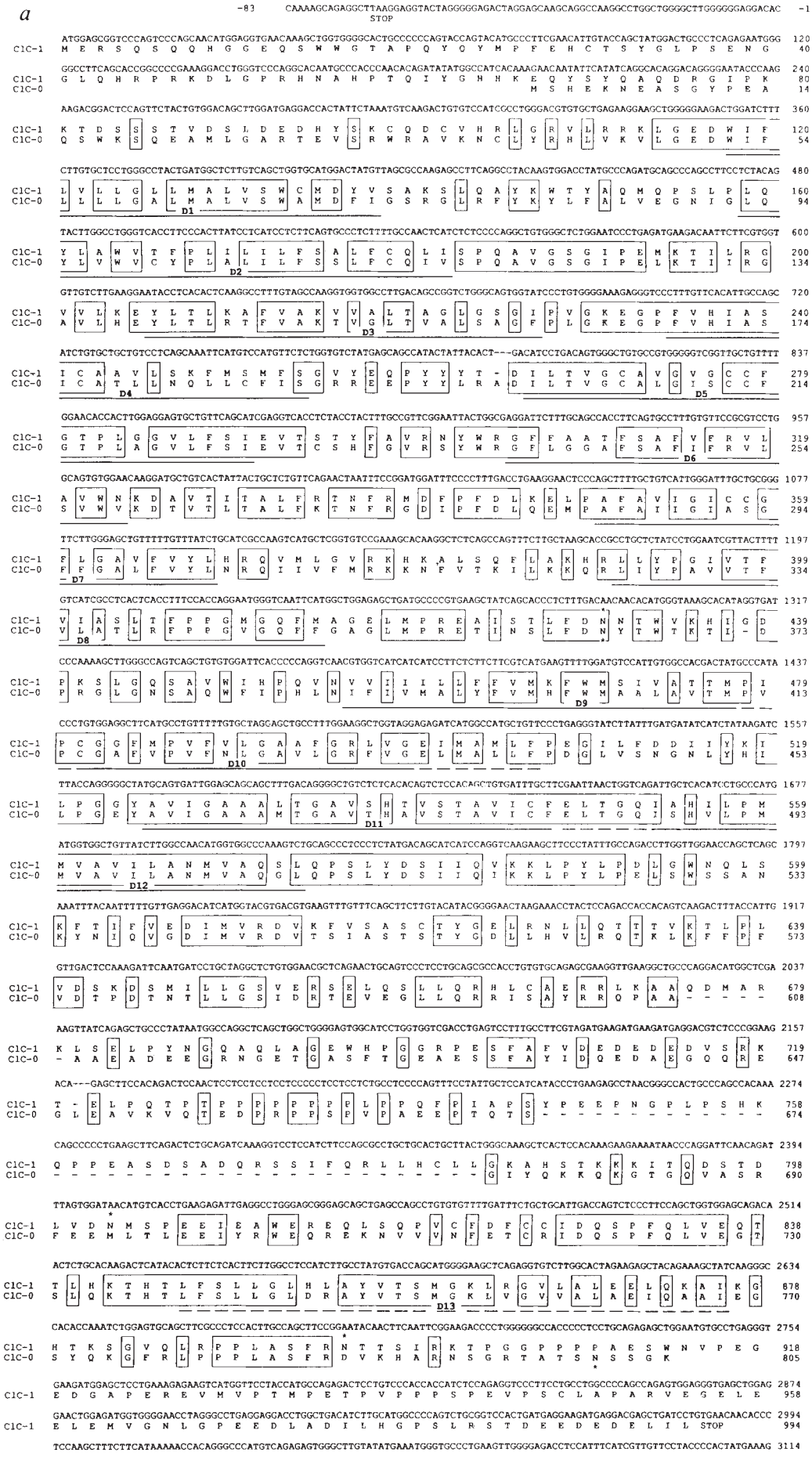

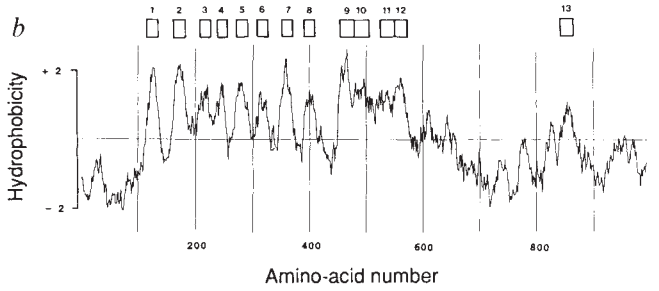

◀ FIG. 1 Sequence and structural prediction for the rat skeletal muscle chloride channel (ClC-1). *a*, Nucleotide sequence of ClC-1 and alignment of its deduced amino-acid sequence (single-letter code) with that of the Cl^- channel from *T. marmorata* electroplax (ClC-0). The initiator methionine was assigned to the first ATG downstream of a stop codon in the frame. It is surrounded by sequences suitable for eukaryotic initiation of translation[22]. The first nucleotide and amino acid of the translation start are designated as position 1. Putative transmembrane domains D1 to D13 are underlined. Identical residues are boxed. Gaps are introduced to maximize alignment. *, Potential *N*-linked glycosylation sites. Compared with ClC-0, the site after D8 is conserved, though it was thought to be cytoplasmic. As in *Torpedo*, another site is found after D13 (but at a different position). An additional site exists between D12 and D13. A consensus phosphorylation site for kinase A (Ser 682) is present somewhat downstream compared with *Torpedo*. A striking feature of the segment between D12 and D13 is a highly negatively charged stretch (beginning at residue 709) of seven alternate Asp and Glu residues followed by a cluster of Pro residues. *b*, Hydrophobicity analysis of the rat skeletal muscle chloride channel protein. The mean hydrophobic index of a nonadecapeptide was calculated[8] and plotted as a function of amino-acid number. Putative membrane-spanning domains are indicated by boxes and numbered from 1–13.

METHODS. An oligo (dT)-primed λgt10 cDNA library from rat skeletal muscle (Clontech) was screened with radiolabelled *T. marmorata* Cl^--channel clone 7I34 (ref. 4) under reduced stringency (25% formamide, 5×SSC, 5× Denhardt's and 0.1% SDS at 42 °C). Additional clones were obtained by rescreening under high-stringency conditions. The complete sequence of ClC-1 was obtained from four overlapping partial cDNA clones (clones λm59, λm49, λm13 and λm26). Both strands were completely sequenced with T7 DNA polymerase (Pharmacia). Partial sequence was also obtained from other independent clones. It is identical to the one shown, with the following exceptions: clone λm30 has a T instead of a C at position 1,724, changing the amino acid from P to L; and λm14 has a T instead of a C at position 1,055, changing an A to a V. The sequence has been deposited in the EMBL/Genbank database (accession number X62894).

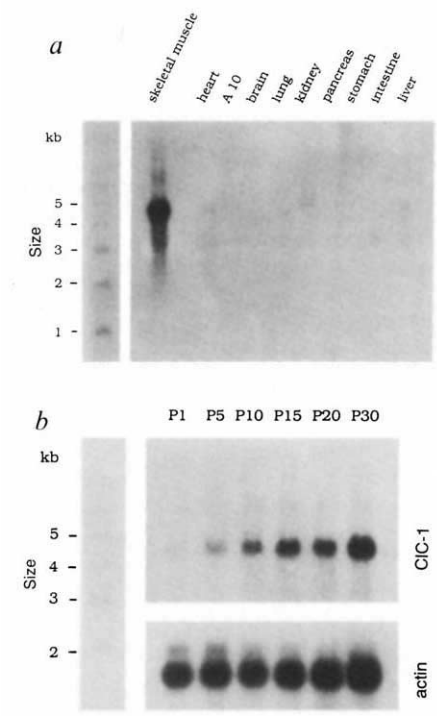

FIG. 2 Tissue distribution and developmental induction of chloride channel ClC-1. *a*, Expression of ClC-1 mRNA in different adult rat tissues as determined by northern analysis. Fragment lengths of a denatured ^{32}P-labelled DNA size standard (BRL) are shown on the left. *b*, Changes in ClC-1 mRNA amounts during skeletal muscle development. Northern analysis of mRNA isolated from rat skeletal muscle taken 1, 5, 10, 15, 20 and 30 days after birth (labelled P1 to P30) is shown. Lower part shows hybridization with γ-actin of the same blot to control for equal loading and absence of degradation.

METHODS. RNA was isolated from different rat tissues and A10 cells (a rat aorta smooth muscle cell line (ATCC CRL 1476)[9] and enriched for poly(A) tracts. Poly(A)$^+$ RNA (10 μg per lane) was electrophoresed on 1% agarose gels containing formaldehyde, blotted and analysed using a full-length ClC-1 probe and standard techniques. Absence of degradation and equal amount of loading was tested by staining with ethidium bromide and control hybridization with γ-actin.

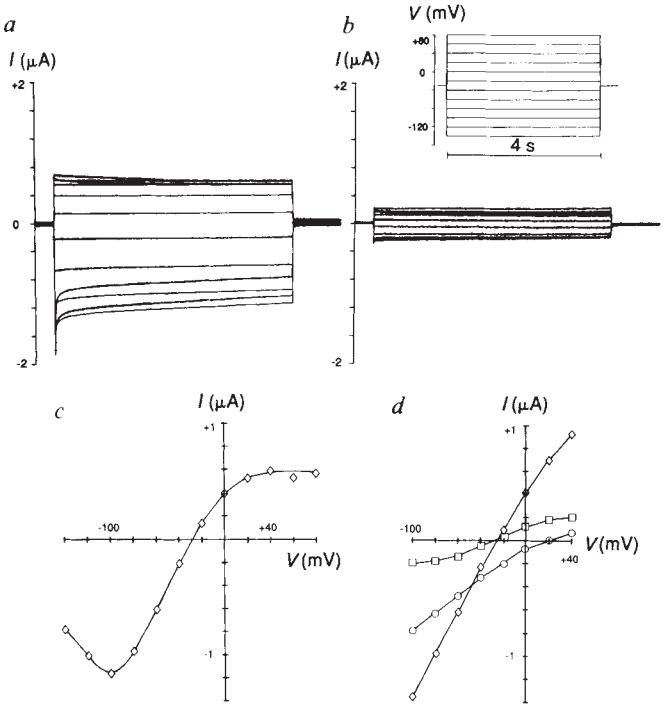

FIG. 3 Functional expression of ClC-1 chloride channel in *Xenopus* oocytes. a, b, Standard two-electrode voltage clamp traces from oocytes previously injected with ClC-1 cRNA. *a*, Oocyte measured in normal saline (ND96)[23]. *b*, The same oocyte measured about 15 min after bath application of 0.1 mM 9-AC. Inhibition by 9-AC needed several minutes to fully develop and was faster at higher concentrations. Inset (above *b*), voltage-clamp programme. From a holding potential of −30 mV, voltage was clamped for intervals of 4 s each to values between +80 and −140 mV. Superimposed traces in *a* and *b* represent currents injected into oocytes. *c*, Quasi-steady-state current–voltage relationship taken from experiment in *a* after a clamp time of 4 s. *d*, Current–voltage relationships of a different oocyte in normal saline ND96 (containing 103 mM Cl^-) (◇), about 15 min after application of 0.1 mM 9-AC (□) and in low-chloride ND96 (7 mM Cl^-, 96 mM cyclamate$^-$) (○).

METHODS. A full-length ClC-1 cDNA clone (F3) was assembled by ligating the 5′ clone λm59 at a *Ssp*I site (at base pair (bp) 205) to clone λm49, followed by ligation to clone λm13 at a *Bsp*EI site (bp 1,010), and then to λm26 (which extends beyond the stop codon at position 2,983) at the *Sal*I site (2,099 bp). As cRNA from that construct could not be expressed in oocytes, we used recombinant polymerase chain reaction (PCR)[24] to replace the muscle 5′ untranslated sequence by 5′ untranslated sequence derived from ClC-0 clone 7I34 (ref. 4). This does not change any amino acid. The sequence of the fragment generated by PCR (ligated to F3 at the bp 205 *Ssp*I site) was fully verified. Capped cRNA was synthesized from this construct using T3 RNA polymerase after linearization of the construct. *Xenopus laevis* oocytes were prepared and injected[23] with 5–10 ng cRNA and measured 2 days later by two-electrode voltage clamp using pClamp software. The holding potential of −30 mV (chosen to be close to the resting voltage and chloride equilibrium potential) was constantly applied during the intervals (20 s) between individual voltage pulses.

steps initially elicit large currents, which then decay rapidly. The rate of deactivation increases with hyperpolarization. In this voltage range, steady-state currents actually decrease with hyperpolarization after passing through a maximum near −100 mV (Fig. 3*c*). Both observations agree remarkably well with studies on macroscopic skeletal muscle Cl^- conductance[1,16]. Currents are predominantly carried by Cl^-, as partial replacement of extracellular Cl^- by impermeant cyclamate$^-$ reduces overall current and shifts the reversal potential ($I = 0$) towards the new Cl^--equilibrium potential (Fig. 3*d*). Further, conductance is >80% inhibited by 0.1 mM 9-anthracene-carboxylic acid (9-AC) (Fig. 3*c*, *d*), a Cl^--channel inhibitor. Similar observations were made with macrosopic muscle Cl^- conductance, where application of 9-AC elicits myotonia[2,3].

There are several functional differences between this and the *Torpedo* channel, one being the sensitivity of 9-AC (ClC-0 is inhibited <50% by 2 mM 9-AC (T.J.J. and G. Schwarz, unpublished results). Although a decrease in open-probability at negative voltages, as observed with ClC-0, may also explain the current decrease with hyperpolarization for ClC-1, probably the most conspicuous difference is the lack of slow channel activation by hyperpolarization observed with ClC-0 (ref. 4). For ClC-0, this reflects a slow opening of a gate operating on both protochannels of the double-barrelled channel[5,17–19]. Whether this implies that ClC-1 has no double-barrelled structure remains to be elucidated in single-channel studies. This is especially important as most patch-clamp studies on muscle Cl^- channels were done on undifferentiated myotubes[20,21] whereas there are no single-channel data on the major Cl^- channel from intact differentiated muscle cells.

Thus the muscle Cl^- channel ClC-1, although in some regions highly homologous to the *Torpedo* channel ClC-0, has distinct electrophysiological properties. This channel is rather specifically expressed in skeletal muscle and probably provides the major Cl^- conductance in that tissue. Its importance for muscle function is best illustrated by the fact that its destruction in mouse mutants leads to myotonia[7]. □

Received 31 July; accepted 27 September 1991.

1. Bretag, A. H. *Physiol. Rev.* **67,** 618–724 (1987).
2. Rüdel, R. & Lehmann-Horn, F. *Physiol. Rev.* **65,** 310–356 (1985).
3. Bryant, S. H. & Morales-Aguilera, A. *J. Physiol., Lond.* **219,** 367–383 (1971).
4. Jentsch, T. J., Steinmeyer, K. & Schwarz, G. *Nature* **348,** 510–514 (1990).
5. Miller, C. & Richard, E. A. in *Chloride Channels and Carriers in Nerve, Muscle, and Glial Cells* (eds Alvarez-Leefsmans, F. J. & Russel, J. M.) 383–405 (Plenum, New York, 1990).
6. Conte Camerino, D., De Luca, A., Mambrini, M. & Vrbovà, G. *Pflügers Arch.* **413,** 568–570 (1989).
7. Steinmeyer, K. *et al. Nature* **354,** 304–308 (1991).
8. Kyte, J. & Doolittle, R. F. *J. molec. Biol.* **157,** 105–132 (1982).
9. Kimes, B. W. & Brandt, B. L. *Expl Cell Res.* **98,** 349–366 (1976).
10. Cooperman, S. S. *et al. Proc. natn. Acad. Sci. U.S.A.* **84,** 8721–8725 (1987).
11. Trimmer, J. S. *et al. Neuron* **3,** 33–49 (1989).
12. Trimmer, J. S., Cooperman, S. S., Agnew, W. S. & Mandel, G. *Devl Biol.* **142,** 360–367 (1990).
13. Kallen, R. L. *et al. Neuron* **4,** 233–242 (1990).
14. Mishina, M. *et al. Nature* **321,** 406–411 (1986).
15. Witzemann, V., Barg, B., Criado, M., Stein, E. & Sakmann, B. *FEBS Lett.* **242,** 419–424 (1989).
16. Palade, P. T. & Barchi, R. L. *J. gen. Physiol.* **69,** 325–342 (1977).
17. Miller, C. *Phil. Trans. R. Soc.* B **299,** 401–411 (1982).
18. Miller, C. & White, M. M. *Proc. natn. Acad. Sci. U.S.A.* **81,** 2772–2775 (1984).
19. Bauer, C. K., Steinmeyer, K., Schwarz, J. R. & Jentsch, T. J. *Proc. natn. Acad. Sci. U.S.A.* (in the press).
20. Blatz, A. L. & Magleby, K. L. *Biophys. J.* **43,** 237–241 (1983).
21. Blatz, A. L. & Magleby, K. L. *Biophys. J.* **47,** 119–123 (1985).
22. Kozak, M. *Nucleic Acids Res.* **12,** 857–872 (1984).
23. Colman, A. in *Transcription and Translation* (eds Hames, B. D. & Higgins, S. J.) 271–302 (IRL, Oxford, 1984).
24. Higuchi, R. in *PCR Technology* (ed. Erlich, H. A.) 61–70 (Stockton, New York, 1989).

ACKNOWLEDGEMENTS. We thank C. Schmekal for technical assistance. This work is supported, in part, by the BMFT, the US Cystic Fibrosis Foundation, the US Muscular Dystrophy Association and the Deutsche Forschungsgemeinschaft.

Inactivation of muscle chloride channel by transposon insertion in myotonic mice

Klaus Steinmeyer*, Rainer Klocke†, Christoph Ortland*, Monika Gronemeier†, Harald Jockusch†, Stefan Gründer* & Thomas J. Jentsch*‡

* Centre for Molecular Neurobiology (ZMNH), Hamburg University, Martinistrasse 52, D-2000 Hamburg 20, Germany
† Developmental Biology Unit, W7, Bielefeld University, PO Box 8640, D-4800 Bielefeld 1, Germany

MYOTONIA (stiffness and impaired relaxation of skeletal muscle) is a symptom of several diseases caused by repetitive firing of action potentials in muscle membranes[1]. Purely myotonic human diseases are dominant myotonia congenita (Thomsen) and recessive generalized myotonia (Becker), whereas myotonic dystrophy is a systemic disease. Muscle hyperexcitability was attributed to defects in sodium channels[2,3] and/or to a decrease in chloride conductance (in Becker's myotonia[4] and in genetic animal models[5–10]). Experimental blockage of Cl^- conductance (normally 70–85% of resting conductance in muscle[11]) in fact elicits myotonia[1,9]. ADR (ref. 12) mice are a realistic animal model[5–7,12–18] for recessive autosomal myotonia. In addition to Cl^- conductance[5], many other parameters[6,12,16] are changed in muscles of homozygous animals. We have now cloned the major mammalian skeletal muscle chloride channel (ClC-1)[19]. Here we report that in ADR mice a transposon of the *ETn* family[20–23] has inserted into the corresponding gene, destroying its coding potential for several membrane-spanning domains. Together with the lack of recombination between the *Clc-1* gene and the *adr* locus, this strongly suggests a lack of functional chloride channels as the primary cause of mouse myotonia.

We first investigated whether in myotonic mice changes in the muscle chloride channel gene can be detected by genomic Southern analysis (Fig. 1). Using a rat muscle Cl^- channel (ClC-1)[19] probe, aberrant fragments were indeed found in ADR (*adr*/*adr*) mice with several restriction nucleases, and with one enzyme in myotonic mice carrying the allelic mutation adr^{mto} (ref. 24). No rearrangement was found with the adr^K (ref. 25) allele. With ADR, aberrant fragments were always larger than the wild-type fragment, suggesting an insertional mutation. A total of 55 ADR mice were tested. In each of these the 6.6-kilobase (kb) *Eco*RI fragment was replaced by the 10.5-kb fragment, which was never found in any homozygous wild-type laboratory mouse. In proven heterozygous A2G mice, both the 6.6- and the 10.5-kb fragments were present.

Northern analysis was used to examine Cl^- channel messenger RNAs in various myotonic mouse strains. A probe from the 5′ end of ClC-1 detected a roughly 4.5-kb message in skeletal muscle of both normal mice and myotonic mice homozygous for adr^{mto} and adr^K, whereas several bands were apparent with *adr*/*adr* mice (a roughly 7–8-kb doublet, and another doublet at about 1.6–2.0 kb) (Fig. 2*a*, *d*). Heterozygous (phenotypically normal) mice (*adr*/+) additionally had normal transcripts (about 4.5 kb), which were missing in homozygous (*adr*/*adr*) muscle. The sizes of the small mRNAs (1.6–2.0 kb) are insufficient to encode a functional Cl^- channel[19,26]. To examine the *adr* mutation in detail, a complementary DNA library from (*adr*/*adr*) skeletal muscle was screened with ClC-1 cDNAs[19]. All 11 clones isolated were homologous to the rat muscle Cl^--channel cDNA 5′ to the sequence encoding the ninth putative

‡ To whom correspondence should be addressed.